

Superposition of Scalar and Residual Dipolar Couplings: Analytical Transfer Functions for Three Spins 1/2 under Cylindrical Mixing Conditions

Burkhard Luy* and Steffen J. Glaser†

*Center of Advanced Research in Biotechnology, 9600 Gudelsky Drive, Rockville, Maryland 20850; and †Institut für Organische Chemie und Biochemie II, Technische Universität München, Lichtenbergstrasse 4, D-85747 Garching, Germany

Received July 10, 2000; revised August 16, 2000

The superposition of scalar and residual dipolar couplings gives rise to so-called cylindrical mixing Hamiltonians in dipolar coupling spectroscopy. General analytical polarization and coherence transfer functions are presented for three cylindrically coupled spins 1/2 under energy-matched conditions. In addition, the transfer efficiency is analyzed as a function of the relative coupling constants for characteristic special cases. © 2001 Academic Press

Key Words: Hartmann–Hahn transfer; residual dipolar couplings; analytical transfer functions; TOCSY; DCOSY.

INTRODUCTION

Homonuclear and heteronuclear coherence and polarization transfer under energy-matched conditions is an important tool in both liquid and solid state NMR (1–9). Such homonuclear and heteronuclear Hartmann–Hahn type experiments can be classified according to the form of the coupling tensors in the effective mixing Hamiltonian (9, 10). For example, isotropic coupling tensors are created by heteronuclear isotropic mixing sequences (9, 11, 12) and by most homonuclear Hartmann–Hahn sequences if applied to scalar coupled spin systems (5, 6, 9). Effective planar coupling tensors (13) are typical for most heteronuclear Hartmann–Hahn experiments (1, 7, 9) and for homonuclear Hartmann–Hahn experiments that are based on RF irradiation at multiple frequencies (14–19). Recently, residual dipolar couplings of partially ordered systems have found wide use in high-resolution NMR of biomolecules (20–23). The simultaneous presence of isotropic couplings and residual dipolar couplings can give rise to a large variety of effective coupling tensors.

In principle, polarization and coherence transfer functions that describe the dynamics of polarization and coherence transfer can be simulated numerically for arbitrary coupling tensors (8, 9, 24–31). However, analytical transfer functions are also highly desirable in order to understand the characteristic transfer dynamics. For a two-spin system, analytical coherence and polarization transfer functions are known for a large range of practically relevant effective coupling tensors (9, 23, 32, 33). For three-spin systems with arbitrary coupling constants, ana-

lytical transfer functions have been derived for isotropic, planar, and dipolar effective coupling tensors (19, 34, 35). For spin systems consisting of four coupled spins 1/2 with arbitrary coupling constants, analytical transfer functions are only known for isotropic mixing experiments (36, 37). In homonuclear Hartmann–Hahn experiments of partially oriented samples (23), the size of scalar coupling constants is typically of the same order of magnitude as the size of the residual dipolar couplings. The class of effective coupling tensors created by the simultaneous presence of isotropic and dipolar couplings corresponds to the anisotropic Ising–Heisenberg model (38) and has also been denoted cylindrical coupling (33). For two cylindrically coupled spins 1/2, the derivation of analytical transfer functions (9, 23, 33) is relatively simple because all terms of the coupling Hamiltonian mutually commute. However, this is not the case for more than two cylindrically coupled spins. In the following, analytical polarization and coherence transfer functions are presented for spin systems consisting of three spins 1/2 under general cylindrical mixing condition with arbitrary coupling constants. In addition, the efficiency of polarization and coherence transfer is analyzed for a number of characteristic coupling topologies.

TWO-SPIN CASE

For a two-spin system the anisotropic Ising–Heisenberg (38) or cylindrical (33) coupling term can be expressed in the form (10)

$$\mathcal{H}_{\text{cyl}} = 2\pi J^{\text{P}}(I_x S_x + I_y S_y) + 2\pi J^{\text{L}} I_z S_z, \quad [1]$$

with the planar and longitudinal coupling constants J^{P} and J^{L} , respectively. For $J^{\text{P}} = 0$ Eq. [1] reduces to the longitudinal coupling term $2\pi J^{\text{L}} I_z S_z$ (9, 10) that is characteristic for the weak coupling limit and that corresponds to the coupling term of the standard Ising model Hamiltonian (38–40). For $J^{\text{L}} = 0$ the coupling term \mathcal{H}_{cyl} represents a planar mixing Hamiltonian (9, 10, 13) which corresponds to the coupling terms in the XY model (42). For $J^{\text{L}} = J^{\text{P}}$ the coupling term \mathcal{H}_{cyl} represents an

isotropic mixing Hamiltonian (5, 9, 11, 12) which corresponds to the coupling term in the Heisenberg or Heisenberg–Dirac–Van Vleck model Hamiltonian (41, 43). For $J^L = -2J^P$ the Hamiltonian \mathcal{H}_{cyl} represents a dipolar coupling term (44).

The combination of an (effective) isotropic coupling term $\mathcal{H}_{\text{iso}} = 2\pi J\{I_x S_x + I_y S_y + I_z S_z\}$ and an (effective) dipolar coupling term of the form $\mathcal{H}_{\text{dip}} = 2\pi D\{2I_z S_z - I_x S_x - I_y S_y\}$ also results in a cylindrical mixing Hamiltonian \mathcal{H}_{cyl} in the form of Eq. [1] with

$$J^L = J + 2D, \quad J^P = J - D. \quad [2]$$

For a two-spin system the coherence and polarization transfer functions for cylindrical mixing can be derived in a straightforward way (9, 23, 33). A summary of the relevant transfer functions using the above nomenclature is given in Table 1. For a longitudinal initial operator $A = I_z$, the transfer functions are independent of the longitudinal coupling constant J^L because the coupling term $2\pi J^L I_z S_z$ commutes both with I_z and with $2\pi J^P (I_x S_x + I_y S_y)$. On the other hand, transfer functions for the transverse initial operators $A = I_x$ or I_y depend on both J^P and J^L . This is illustrated in Fig. 1 where characteristic transfer functions $T_{I_z \rightarrow S_z}$ and $T_{I_x \rightarrow S_x}$ are shown.

THREE-SPIN CASE

For a spin system consisting of three coupled spins 1/2, the anisotropic Ising–Heisenberg or cylindrical mixing Hamiltonian has the form

$$\mathcal{H}_{\text{cyl}} = 2\pi \sum_{i<j}^3 J_{ij}^P \{I_{ix} I_{jx} + I_{iy} I_{jy}\} + 2\pi \sum_{i<j}^3 J_{ij}^L I_{iz} I_{jz}, \quad [3]$$

with the effective planar and longitudinal coupling constants J_{ij}^P and J_{ij}^L , respectively. In analogy to the case of three coupled spins under planar or dipolar mixing conditions, polarization transfer functions can be determined if the eigenvalues and eigenfunctions of \mathcal{H}_{cyl} are known (19, 35). As \mathcal{H}_{cyl} commutes with $F_z = I_{1z} + I_{2z} + I_{3z}$, the mixing Hamiltonian assumes a

TABLE 1

Coherence and Polarization Transfer Functions $T_{A \rightarrow B}$ for Two Spins I and S under Cylindrical Mixing Conditions

$T_{I_x \rightarrow I_x} = T_{I_y \rightarrow I_y} = 1 - \sin(\pi J^L \tau) \sin(\pi J^P \tau)$
$T_{I_z \rightarrow I_z} = 1 - \sin^2(\pi J^P \tau)$
$T_{I_x \rightarrow S_x} = T_{I_y \rightarrow S_y} = \sin(\pi J^L \tau) \sin(\pi J^P \tau)$
$T_{I_z \rightarrow S_z} = \sin^2(\pi J^P \tau)$
$T_{I_y \rightarrow 2I_x S_z} = -T_{I_x \rightarrow 2I_y S_z} = \frac{1}{2} \{\sin(\pi(J^L + J^P)\tau) + \sin(\pi(J^L - J^P)\tau)\}$
$T_{I_x \rightarrow 2I_y S_y} = -T_{I_y \rightarrow 2I_x S_x} = \frac{1}{2} \{\sin(\pi(J^L + J^P)\tau) - \sin(\pi(J^L - J^P)\tau)\}$
$T_{I_z \rightarrow 2I_x S_x} = -T_{I_z \rightarrow 2I_y S_y} = \frac{1}{2} \sin(2\pi J^P \tau)$

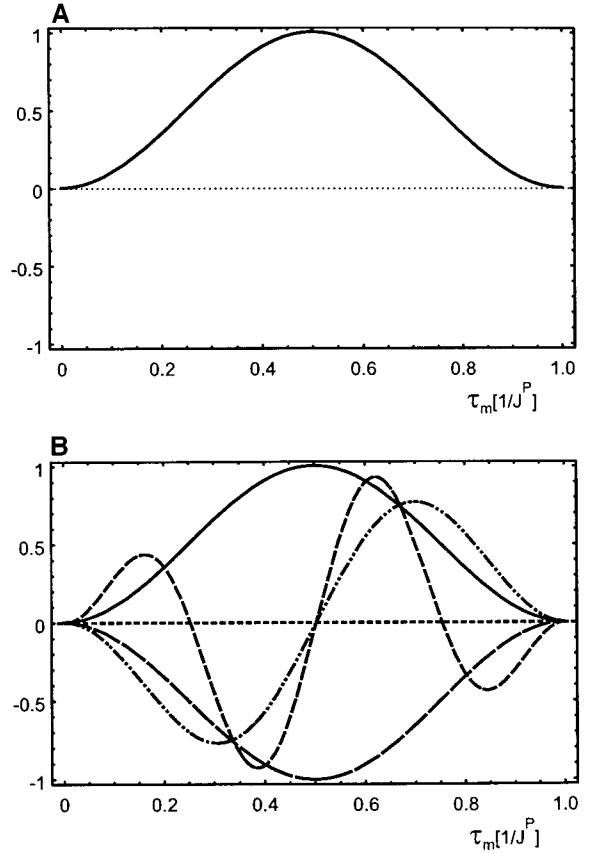


FIG. 1. Polarization and coherence transfer functions of a two-spin system under various cylindrical mixing conditions (see Eq. [1]). (A) The polarization transfer function $T_{I_z \rightarrow S_z}$ is independent of J^L and only depends on the planar coupling constant J^P . (B) In contrast, the coherence transfer functions $T_{I_x \rightarrow S_x} = T_{I_y \rightarrow S_y}$ depend not only on J^P but also on J^L . The curves represent characteristic coherence transfer functions for $J^L = -2J^P$ (dipolar mixing, - · - · -), $J^L = -J^P$ (— · —), $J^L = 0$ (planar mixing, - - -), $J^L = J^P$ (isotropic mixing, —), and $J^L = 4J^P$ (· · · · ·).

block structure in the basis of the product functions $|\alpha\alpha\alpha\rangle$ (with magnetic quantum number $m = 3/2$), $|\beta\alpha\alpha\rangle$, $|\alpha\beta\alpha\rangle$, $|\alpha\alpha\beta\rangle$ (with $m = 1/2$), $|\alpha\beta\beta\rangle$, $|\beta\alpha\beta\rangle$, $|\beta\beta\alpha\rangle$ (with $m = -1/2$), and $|\beta\beta\beta\rangle$ (with $m = -3/2$). Each block only connects product functions with equal magnetic quantum number m . For $m = \pm 3/2$, the resulting 1×1 blocks are

$$\mathcal{H}_{\text{cyl}}^{(3/2)} = \mathcal{H}_{\text{cyl}}^{(-3/2)} = \frac{\pi}{2} (J_{12}^L + J_{13}^L + J_{23}^L) = \lambda_0, \quad [4]$$

where λ_0 corresponds to two degenerate eigenvalues of \mathcal{H}_{cyl} . For $m = \pm 1/2$, the blocks have the form

$$\mathcal{H}_{\text{cyl}}^{(1/2)} = \mathcal{H}_{\text{cyl}}^{(-1/2)} = \pi \begin{pmatrix} \Sigma_1 & J_{12}^P & J_{13}^P \\ J_{12}^P & \Sigma_2 & J_{23}^P \\ J_{13}^P & J_{23}^P & \Sigma_3 \end{pmatrix}, \quad [5]$$

with

$$\Sigma_i = \frac{J_{jk}^L - J_{ij}^L - J_{ik}^L}{2} \quad [6]$$

for $\{ijk\} = \{123\}$, $\{231\}$, and $\{312\}$ and with $J_{ij}^L = J_{ji}^L$ and $J_{ij}^P = J_{ji}^P$. The eigenvalues of these 3×3 matrices can be found using Cardan's formula (45):

$$\begin{aligned} \lambda_1 &= -\frac{\lambda_0}{3} + 4\pi \sqrt{\frac{|p|}{3}} \cos\left(\frac{\varphi}{3}\right) \\ \lambda_{2,3} &= -\frac{\lambda_0}{3} - 4\pi \sqrt{\frac{|p|}{3}} \cos\left(\frac{\varphi \mp \pi}{3}\right), \end{aligned} \quad [7]$$

with

$$\varphi = \arccos\left(\frac{-q}{2\sqrt{\frac{|p|}{3}}}\right), \quad [8]$$

$$p = \frac{1}{12} \sum_{i < j}^3 \Sigma_i \Sigma_j - (\Sigma_i)^2 - 3(J_{ij}^P)^2$$

and

$$\begin{aligned} q &= \frac{1}{3} \left\{ J_{12}^P \Sigma_3 + J_{13}^P \Sigma_2 + J_{23}^P \Sigma_1 - \frac{1}{4} J_{12}^P J_{13}^P J_{23}^P - \frac{1}{3} \Sigma_1 \Sigma_2 \Sigma_3 \right. \\ &\quad \left. + \sum_{i \neq j}^3 \Sigma_i \left(\frac{8}{3} \Sigma_i \Sigma_j - \frac{1}{2} J_{ij}^P \right) - \frac{1}{36} \sum_i (\Sigma_i)^3 \right\}. \end{aligned} \quad [9]$$

For each eigenvalue λ_i (Eq. [7]) the three components α_i , β_i , and γ_i of the corresponding normalized eigenvectors are given by

$$\alpha_i = c_i^{(123)}/n_i, \quad \beta_i = c_i^{(231)}/n_i, \quad \gamma_i = c_i^{(312)}/n_i, \quad [10]$$

with

$$\begin{aligned} c_i^{(lmn)} &= J_{mn}^P (J_{mn}^P - J_{lm}^P - J_{ln}^P) - \Sigma_m \Sigma_n + \Sigma_m J_{ln}^P + \Sigma_n J_{lm}^P \\ &\quad + (\Sigma_m - J_{lm}^P + \Sigma_n - J_{ln}^P)(\lambda_i/\pi) - (\lambda_i/\pi)^2 \end{aligned} \quad [11]$$

and

$$n_i = \sqrt{(c_i^{(123)})^2 + (c_i^{(231)})^2 + (c_i^{(312)})^2}. \quad [12]$$

In special cases (e.g., for isotropic mixing with $J_{ij}^P = J_{ij}^L$) when $c_1^{(lmn)} = c_2^{(lmn)} = c_3^{(lmn)} = 0$ for all combinations (lmn) , Eq. [11] is to be replaced by

$$c_i^{(123)} = \Sigma_2 J_{13}^P - J_{12}^P J_{23}^P - J_{13}^P (\lambda_i/\pi)$$

$$c_i^{(231)} = \Sigma_1 J_{23}^P - J_{12}^P J_{13}^P - J_{23}^P (\lambda_i/\pi)$$

$$c_i^{(312)} = (J_{12}^P)^2 - \Sigma_1 \Sigma_2 + (\Sigma_1 + \Sigma_2)(\lambda_i/\pi) - (\lambda_i/\pi)^2.$$

[13]

Equations [10]–[13] represent the eigenvector components in all cases where the eigenvalues (Eq. [7]) are nondegenerate i.e., $\lambda_1 \neq \lambda_2 \neq \lambda_3 \neq \lambda_1$. In the practical calculation of transfer functions this can always be achieved by a slight variation of the coupling constants. Based on the components of the eigenvectors (Eq. [10]), an orthonormal eigenbasis of the mixing Hamiltonian \mathcal{H}_{cyl} is given by

$$\psi_1 = |\alpha\alpha\alpha\rangle$$

$$\psi_2 = \alpha_1 |\beta\alpha\alpha\rangle + \beta_1 |\alpha\beta\alpha\rangle + \gamma_1 |\alpha\alpha\beta\rangle$$

$$\psi_3 = \alpha_2 |\beta\alpha\alpha\rangle + \beta_2 |\alpha\beta\alpha\rangle + \gamma_2 |\alpha\alpha\beta\rangle$$

$$\psi_4 = \alpha_3 |\beta\alpha\alpha\rangle + \beta_3 |\alpha\beta\alpha\rangle + \gamma_3 |\alpha\alpha\beta\rangle$$

$$\psi_5 = \alpha_1 |\alpha\beta\beta\rangle + \beta_1 |\beta\alpha\beta\rangle + \gamma_1 |\beta\beta\alpha\rangle$$

$$\psi_6 = \alpha_2 |\alpha\beta\beta\rangle + \beta_2 |\beta\alpha\beta\rangle + \gamma_2 |\beta\beta\alpha\rangle$$

$$\psi_7 = \alpha_3 |\alpha\beta\beta\rangle + \beta_3 |\beta\alpha\beta\rangle + \gamma_3 |\beta\beta\alpha\rangle$$

$$\psi_8 = |\beta\beta\beta\rangle. \quad [14]$$

In this eigenbasis, transfer functions

$$T_{A \rightarrow B}(\tau) = \frac{\text{Tr}\{B^\dagger U(\tau) A U^\dagger(\tau)\}}{\text{Tr}\{B^\dagger B\}} \quad [15]$$

between two operators A and B can be calculated in a straightforward way because the propagator

$$U(\tau) = \exp\{-i\mathcal{H}_{\text{cyl}}\tau\} \quad [16]$$

is diagonal with $(U)_{11} = (U)_{88} = \exp\{-i\lambda_0\tau\}$, $(U)_{22} = (U)_{55} = \exp\{-i\lambda_1\tau\}$, $(U)_{33} = (U)_{66} = \exp\{-i\lambda_2\tau\}$, and $(U)_{44} = (U)_{77} = \exp\{-i\lambda_3\tau\}$.

With the help of the algebraic program *Mathematica* (46) we derived compact analytical expressions for coherence and polarization transfer functions of practical interest. All nonzero polarization and coherence transfer functions $T_{A \rightarrow B}$ for $A = I_{1z}$ and $A = I_{1x}$ are summarized in Tables 2 and 3, respectively. As the cylindrical mixing Hamiltonian is invariant under rotations around the z axis, the transfer functions $T_{I_{1x} \rightarrow B}$ are identical to the transfer functions $T_{I_{1y} \rightarrow B}$, where the target operator B' is

TABLE 2
Polarization Transfer Functions $T_{I_{kz} \rightarrow B}$ for a Three-Spin System under Cylindrical Mixing Conditions

$$T_{I_{1z} \rightarrow I_{1z}} = T_{11}^z = 1 - \sum_{i < j}^3 \frac{1}{2} w_{ij}^2 \{1 - \cos(\Delta_{ij}\tau)\}$$

$$T_{I_{1z} \rightarrow I_{2z}} = T_{12}^z = \sum_{i < j}^3 \frac{1}{2} \{(\alpha_i \alpha_j - \beta_i \beta_j)^2 - (\gamma_i \gamma_j)^2\} (1 - \cos(\Delta_{ij}\tau))$$

$$T_{I_{1z} \rightarrow I_{3z}} = T_{13}^z = \sum_{i < j}^3 \frac{1}{2} \{(\alpha_i \alpha_j - \gamma_i \gamma_j)^2 - (\beta_i \beta_j)^2\} \{1 - \cos(\Delta_{ij}\tau)\}$$

$$T_{I_{1z} \rightarrow I_{1z} I_{2y} - I_{2z} I_{1y}} = \sum_{i < j}^3 \frac{1}{2} \{(\beta_i \alpha_j - \alpha_i \beta_j) w_{ij}\} \sin(\Delta_{ij}\tau)$$

$$T_{I_{1z} \rightarrow I_{1z} I_{3y} - I_{3z} I_{1y}} = \sum_{i < j}^3 \frac{1}{2} \{(\gamma_i \alpha_j - \alpha_i \gamma_j) w_{ij}\} \sin(\Delta_{ij}\tau)$$

$$T_{I_{1z} \rightarrow I_{2z} I_{3y} - I_{3z} I_{2y}} = \sum_{i < j}^3 \frac{1}{2} \{(\gamma_i \beta_j - \beta_i \gamma_j) w_{ij}\} \sin(\Delta_{ij}\tau)$$

$$T_{I_{1z} \rightarrow I_{1z}(I_{2z} I_{3z} + I_{2y} I_{3y})} = \sum_{i < j}^3 \frac{1}{4} \{(\beta_i \gamma_j + \gamma_i \beta_j) w_{ij}\} \{1 - \cos(\Delta_{ij}\tau)\}$$

$$T_{I_{1z} \rightarrow I_{2z}(I_{1z} I_{3z} + I_{1y} I_{3y})} = \sum_{i < j}^3 \frac{1}{4} \{(\alpha_i \gamma_j + \gamma_i \alpha_j) w_{ij}\} \{1 - \cos(\Delta_{ij}\tau)\}$$

$$T_{I_{1z} \rightarrow I_{3z}(I_{1z} I_{2z} + I_{1y} I_{2y})} = \sum_{i < j}^3 \frac{1}{4} \{(\alpha_i \beta_j + \beta_i \alpha_j) w_{ij}\} \{1 - \cos(\Delta_{ij}\tau)\}$$

Note. α_i , β_i , and γ_i are defined in Eq. [10] and $w_{ij} = \alpha_i \alpha_j - \beta_i \beta_j - \gamma_i \gamma_j$.

related to B by a 90° z rotation. Except for constant terms, all polarization transfer functions $T_{I_{kz} \rightarrow B}$ can be expressed as combinations of three harmonic terms with oscillation frequencies Δ_{12} , Δ_{13} , and Δ_{23} corresponding to differences of the eigenvalues λ_1 , λ_2 , and λ_3 (c.f. Eq. [7]):

$$\Delta_{ij} = \lambda_i - \lambda_j. \quad [17]$$

In the transfer functions $T_{I_{kz} \rightarrow B}$ of transverse magnetization, three additional harmonic terms occur with oscillation frequencies $\Delta_{0i} = \lambda_0 - \lambda_i$ with $i = 1, 2$, and 3 (c.f. Eqs. [4] and [7]).

TRANSFER EFFICIENCIES

Examples of characteristic transfer functions $T_{I_{kz} \rightarrow B}$ and $T_{I_{kx} \rightarrow B}$ are shown in Figs. 2 and 3, respectively. As in Fig. 1, the ratio J_{ij}^L/J_{ij}^P of longitudinal and planar coupling constants was varied between -2 (A–A') and 4 (F–F'). The planar coupling constants were chosen to be $J_{12}^P = -10$ Hz, $J_{13}^P = 4.6$ Hz, and $J_{23}^P = 11$ Hz in order to simplify the comparison with previously presented theoretical (19, 34, 35) and experimental (19, 34) transfer functions. The analytical transfer functions are identi-

cal to simulated transfer functions that were calculated numerically using the program SIMONE (29) (data not shown).

In contrast to the case of two cylindrically coupled spins (cf. Fig. 1A), the transfer of polarization $T_{I_{kz} \rightarrow I_{lz}}$ does depend on the ratio J_{ij}^L/J_{ij}^P of longitudinal and planar coupling constants in the case of three coupled spins (cf. Fig. 2), because the planar and longitudinal coupling terms only commute in the case of two coupled spins but not in the case of three coupled spins. The coherence transfer functions $T_{I_{kx} \rightarrow I_{lx}}$ (see Fig. 3 and Table 3) are in general more complicated than the corresponding polarization transfer functions $T_{I_{kz} \rightarrow I_{lz}}$ (see Fig. 2 and Table 2). Whereas only positive polarization transfer functions $T_{I_{kz} \rightarrow I_{lz}}$ are found for three cylindrically coupled spins $1/2$, the coherence transfer functions $T_{I_{kx} \rightarrow I_{lx}}$ can also become negative, except for the case of isotropic mixing where $T_{I_{kx} \rightarrow I_{lx}} = T_{I_{kz} \rightarrow I_{lz}}$ is always positive (24, 34, 47).

In order to introduce a concise notation for the discussion of the transfer efficiency under various combinations of cylindrical coupling tensors, we rewrite \mathcal{H}_{cyl} (Eq. [3]) in the form (10).

$$\mathcal{H}_{\text{cyl}} = 2\pi \sum_{i < j}^3 J_{ij} \{s_{ij}^P (I_{ix} I_{jx} + I_{iy} I_{jy}) + s_{ij}^L I_{iz} I_{jz}\}, \quad [18]$$

where the planar and longitudinal coupling constants are related to the fictitious coupling constants J_{ij} by $J_{ij}^P = s_{ij}^P J_{ij}$ and $J_{ij}^L = s_{ij}^L J_{ij}$, respectively. In analogy to previous definitions (9, 10, 35) of quality factors that reflect both the amplitude and the duration of the transfer from $I_{k\alpha}$ to $I_{l\alpha}$, we define the transfer efficiency η_{kl}^α for cylindrical mixing as

$$\eta_{kl}^\alpha = \kappa \max_{\tau > 0} \{|T_{I_{k\alpha} \rightarrow I_{l\alpha}}(\tau)| \exp(-\tau |J_{kl}|)\}, \quad [19]$$

where κ is 1 (or -1) if $T_{I_{k\alpha} \rightarrow I_{l\alpha}}(\tau_{\text{max}})$ is positive (or negative) at the mixing time τ_{max} where $|T_{I_{k\alpha} \rightarrow I_{l\alpha}}(\tau)| \exp(-\tau |J_{kl}|)$ assumes its maximum value. For a given set of planar and longitudinal scaling factors $\mathbf{s}^P = \{s_{12}^P, s_{13}^P, s_{23}^P\}$ and $\mathbf{s}^L = \{s_{12}^L, s_{13}^L, s_{23}^L\}$ the transfer efficiency η_{12}^α depends only on the relative coupling constants J_{13}/J_{12} and J_{23}/J_{12} , which makes it possible to plot two-dimensional transfer efficiency maps $\eta_{12}^\alpha(J_{13}/J_{12}, J_{23}/J_{12})$ (10).

Figures 4 and 5 show longitudinal and transverse transfer efficiency maps η_{12}^z and $\eta_{12}^x = \eta_{12}^y$ for a number of characteristic sets of scaling factors \mathbf{s}^P and \mathbf{s}^L . Figures 4A and 5A correspond to the case of isotropic mixing for a two-spin system where $\eta_{12}^z = \eta_{12}^x = 0.62$ (10). In Figs. 4B and 5B, spins 1 and 2 are isotropically coupled whereas spin pairs 1–3 and 2–3 have a purely longitudinal coupling tensor (10). Figures 4C and 5C represent an intermediate case between Figs. 4B and 5B and the case where all three spins are isotropically coupled (Figs. 4E and 5E). Figures 4D–4L and 5D–5L represent a series of longitudinal and transverse transfer efficiency

TABLE 3
Coherence Transfer Functions $T_{I_{1x} \rightarrow B}$ for a Three-Spin System under Cylindrical Mixing Conditions

$$\begin{aligned}
T_{I_{1x} \rightarrow I_{1x}} &= T_{11}^x = \sum_{i=1}^3 \gamma_i^2 \beta_i^2 + \frac{1}{2} \sum_{i=1}^3 \alpha_i^2 \cos(\Delta_{0i}\tau) + \frac{1}{2} \sum_{i=1}^3 \sum_{j=i+1}^3 \nu_{ij}^2 \cos(\Delta_{ij}\tau) \\
T_{I_{1x} \rightarrow I_{2x}} &= T_{12}^x = \sum_{i=1}^3 \gamma_i^2 \beta_i \alpha_i + \frac{1}{2} \sum_{i=1}^3 \beta_i \alpha_i \cos(\Delta_{0i}\tau) + \frac{1}{2} \sum_{i=1}^3 \sum_{j=i+1}^3 \nu_{ij} (\gamma_i \alpha_j + \gamma_j \alpha_i) \cos(\Delta_{ij}\tau) \\
T_{I_{1x} \rightarrow I_{3x}} &= T_{13}^x = \sum_{i=1}^3 \gamma_i \beta_i^2 \alpha_i + \frac{1}{2} \sum_{i=1}^3 \gamma_i \alpha_i \cos(\Delta_{0i}\tau) + \frac{1}{2} \sum_{i=1}^3 \sum_{j=i+1}^3 \nu_{ij} (\beta_i \alpha_j + \beta_j \alpha_i) \cos(\Delta_{ij}\tau) \\
T_{I_{1x} \rightarrow I_{1z} I_{2y}} &= \sum_{i=1}^3 \beta_i \alpha_i \sin(\Delta_{0i}\tau) + \sum_{i=1}^3 \sum_{j=i+1}^3 \nu_{ij} (\gamma_i \alpha_j - \gamma_j \alpha_i) \sin(\Delta_{ij}\tau) \\
T_{I_{1x} \rightarrow I_{2z} I_{1y}} &= \sum_{i=1}^3 \alpha_i^2 \sin(\Delta_{0i}\tau) + \sum_{i=1}^3 \sum_{j=i+1}^3 \nu_{ij} (\gamma_i \beta_j - \gamma_j \beta_i) \sin(\Delta_{ij}\tau) \\
T_{I_{1x} \rightarrow I_{1z} I_{3y}} &= \sum_{i=1}^3 \gamma_i \alpha_i \sin(\Delta_{0i}\tau) + \sum_{i=1}^3 \sum_{j=i+1}^3 \nu_{ij} (\beta_i \alpha_j - \beta_j \alpha_i) \sin(\Delta_{ij}\tau) \\
T_{I_{1x} \rightarrow I_{3z} I_{1y}} &= \sum_{i=1}^3 \alpha_i^2 \sin(\Delta_{0i}\tau) - \sum_{i=1}^3 \sum_{j=i+1}^3 \nu_{ij} (\gamma_i \beta_j - \gamma_j \beta_i) \sin(\Delta_{ij}\tau) \\
T_{I_{1x} \rightarrow I_{2z} I_{3y}} &= \sum_{i=1}^3 \gamma_i \alpha_i \sin(\Delta_{0i}\tau) - \sum_{i=1}^3 \sum_{j=i+1}^3 \nu_{ij} (\beta_i \alpha_j - \beta_j \alpha_i) \sin(\Delta_{ij}\tau) \\
T_{I_{1x} \rightarrow I_{3z} I_{2y}} &= \sum_{i=1}^3 \beta_i \alpha_i \sin(\Delta_{0i}\tau) - \sum_{i=1}^3 \sum_{j=i+1}^3 \nu_{ij} (\gamma_i \alpha_j - \gamma_j \alpha_i) \sin(\Delta_{ij}\tau) \\
T_{I_{1x} \rightarrow I_{1z} I_{2z} I_{3y}} &= 2 \sum_{i=1}^3 \gamma_i \beta_i (\gamma_i^2 + \beta_i^2 - \alpha_i^2) + 2 \sum_{i=1}^3 \sum_{j=i+1}^3 \nu_{ij} (\gamma_i \gamma_j + \beta_i \beta_j - \alpha_i \alpha_j) \cos(\Delta_{ij}\tau) \\
T_{I_{1x} \rightarrow I_{2z} I_{1z} I_{3y}} &= 2 \sum_{i=1}^3 \gamma_i \beta_i (\gamma_i^2 - \beta_i^2 + \alpha_i^2) + 2 \sum_{i=1}^3 \sum_{j=i+1}^3 \nu_{ij} (\gamma_i \gamma_j - \beta_i \beta_j + \alpha_i \alpha_j) \cos(\Delta_{ij}\tau) \\
T_{I_{1x} \rightarrow I_{3z} I_{1z} I_{2y}} &= 2 \sum_{i=1}^3 \gamma_i \beta_i (-\gamma_i^2 + \beta_i^2 + \alpha_i^2) + 2 \sum_{i=1}^3 \sum_{j=i+1}^3 \nu_{ij} (-\gamma_i \gamma_j + \beta_i \beta_j + \alpha_i \alpha_j) \cos(\Delta_{ij}\tau) \\
T_{I_{1x} \rightarrow I_{1z} I_{2z} I_{3z}} &= -4 \sum_{i=1}^3 \gamma_i^2 \beta_i^2 + 2 \sum_{i=1}^3 \alpha_i^2 \cos(\Delta_{0i}\tau) - 2 \sum_{i=1}^3 \sum_{j=i+1}^3 \nu_{ij}^2 \cos(\Delta_{ij}\tau) \\
T_{I_{1x} \rightarrow I_{2z} I_{1z} I_{3z}} &= -4 \sum_{i=1}^3 \gamma_i^2 \beta_i \alpha_i + 2 \sum_{i=1}^3 \beta_i \alpha_i \cos(\Delta_{0i}\tau) - 2 \sum_{i=1}^3 \sum_{j=i+1}^3 \nu_{ij} (\gamma_i \alpha_j + \gamma_j \alpha_i) \cos(\Delta_{ij}\tau) \\
T_{I_{1x} \rightarrow I_{3z} I_{1z} I_{2z}} &= -4 \sum_{i=1}^3 \gamma_i \beta_i^2 \alpha_i + 2 \sum_{i=1}^3 \gamma_i \alpha_i \cos(\Delta_{0i}\tau) - 2 \sum_{i=1}^3 \sum_{j=i+1}^3 \nu_{ij} (\beta_i \alpha_j + \beta_j \alpha_i) \cos(\Delta_{ij}\tau)
\end{aligned}$$

Note. α_i , β_i , and γ_i are defined in Eq. [10] and $\nu_{ij} = (\alpha_i \beta_j + \alpha_j \beta_i)$.

maps where all planar scaling factors are held constant ($s_{kl}^P = 1$) whereas the (identical) longitudinal scaling factors ($s_{12}^L = s_{13}^L = s_{23}^L$) are varied between 5 and -5 . This series includes the ideal cases of isotropic (Figs. 4E and 5E), planar (Figs. 4G and 5G), and dipolar (Figs. 4K and 5K) mixing for three coupled spins 1/2. If the coupling tensors are dominated by longitudinal coupling terms (cf. Figs. 4D, 4L, 5D, and 5L) the transfer of polarization and coherence between the spin pair 1–2 is effectively truncated except for some cases where the

passive couplings J_{13} and J_{23} are approximately identical. Figures 4M–4O and 5M–5O correspond to the cases with (effective) planar coupling terms for spin pairs 1–3 and 2–3 where the coupling tensor for spin pair 1–2 is changed from isotropic (Figs. 4M and 5M) to dipolar (Figs. 4O and 5O) with an intermediate case shown in Figs. 4N and 5N. Corresponding maps are shown in Figs. 4P–4R and 5P–5R, except that here the coupling tensor for spin pair 1–3 is changed from isotropic (Figs. 4P and 5P) to dipolar (Figs. 4R and 5R) while planar

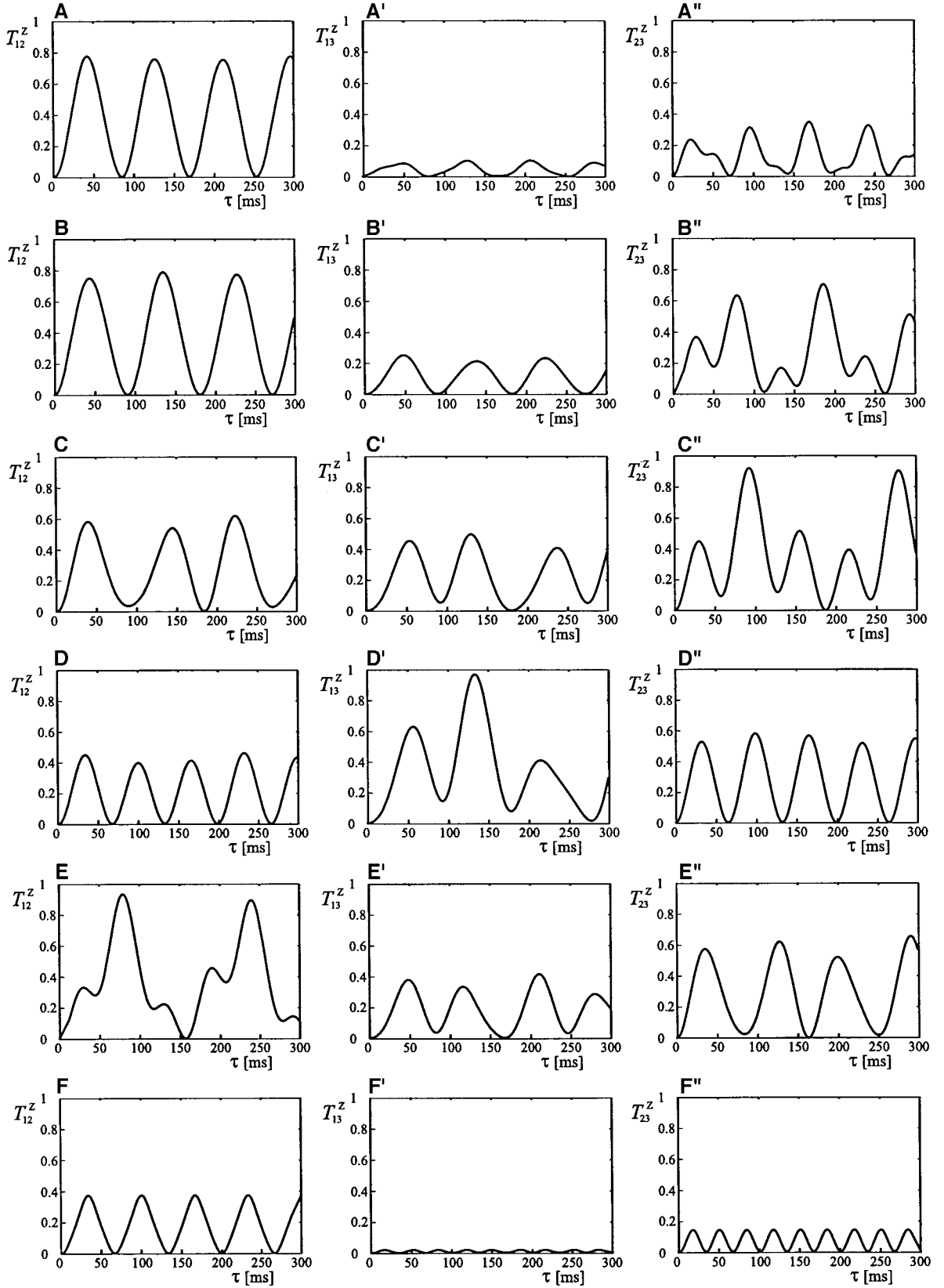


FIG. 2. Polarization transfer functions $T_{ij}^z = T_{I_{iz} \rightarrow J_{jz}}$ of a spin system consisting of three coupled spins $1/2$ with $J_{12}^p = -10$ Hz, $J_{13}^p = 4.6$ Hz, and $J_{23}^p = 11$ Hz under various cylindrical mixing conditions. (A–A'') $J_{ij}^l = -2J_{ij}^p$ (dipolar mixing, cf. (35)), (B–B'') $J_{ij}^l = -J_{ij}^p$, (C–C'') $J_{ij}^l = -\frac{1}{2}J_{ij}^p$, (D–D'') $J_{ij}^l = 0$ (planar mixing, cf. (19)), (E–E'') $J_{ij}^l = J_{ij}^p$ (isotropic mixing, cf. (34)), and (F–F'') $J_{ij}^l = 4J_{ij}^p$.

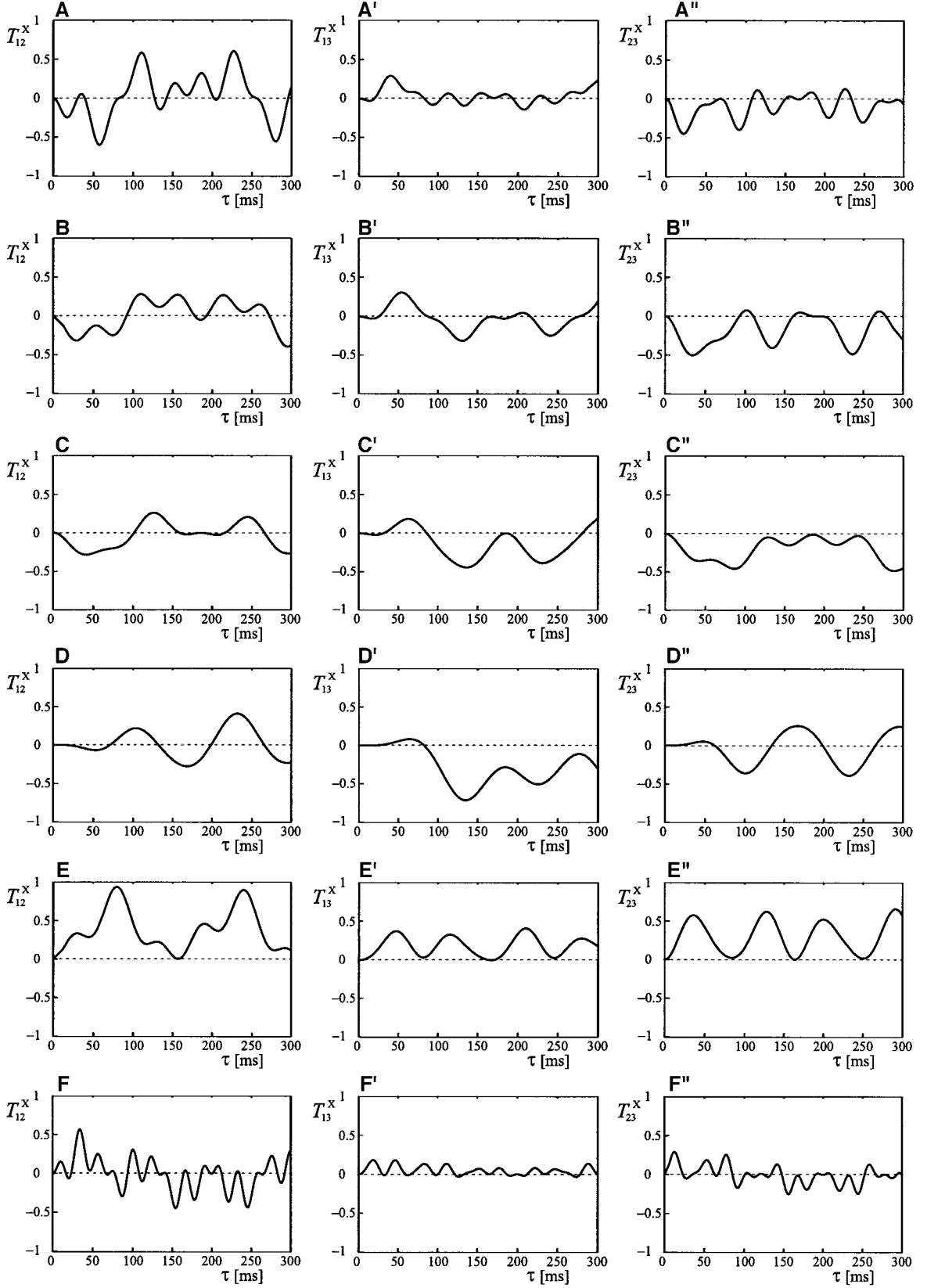


FIG. 3. Coherence transfer functions $T_{ij}^X = T_{I_{ix} \rightarrow I_{jx}}$ of a spin system consisting of three coupled spins $1/2$ with $J_{12}^P = -10$ Hz, $J_{13}^P = 4.6$ Hz, and $J_{23}^P = 11$ Hz under various cylindrical mixing conditions. (A–A'') $J_{ij}^L = -2J_{ij}^P$ (dipolar mixing, cf. (35)), (B–B'') $J_{ij}^L = -J_{ij}^P$, (C–C'') $J_{ij}^L = -\frac{1}{2}J_{ij}^P$, (D–D'') $J_{ij}^L = 0$ (planar mixing), (E–E'') $J_{ij}^L = J_{ij}^P$ (isotropic mixing, cf. (34)), and (F–F'') $J_{ij}^L = 4J_{ij}^P$.

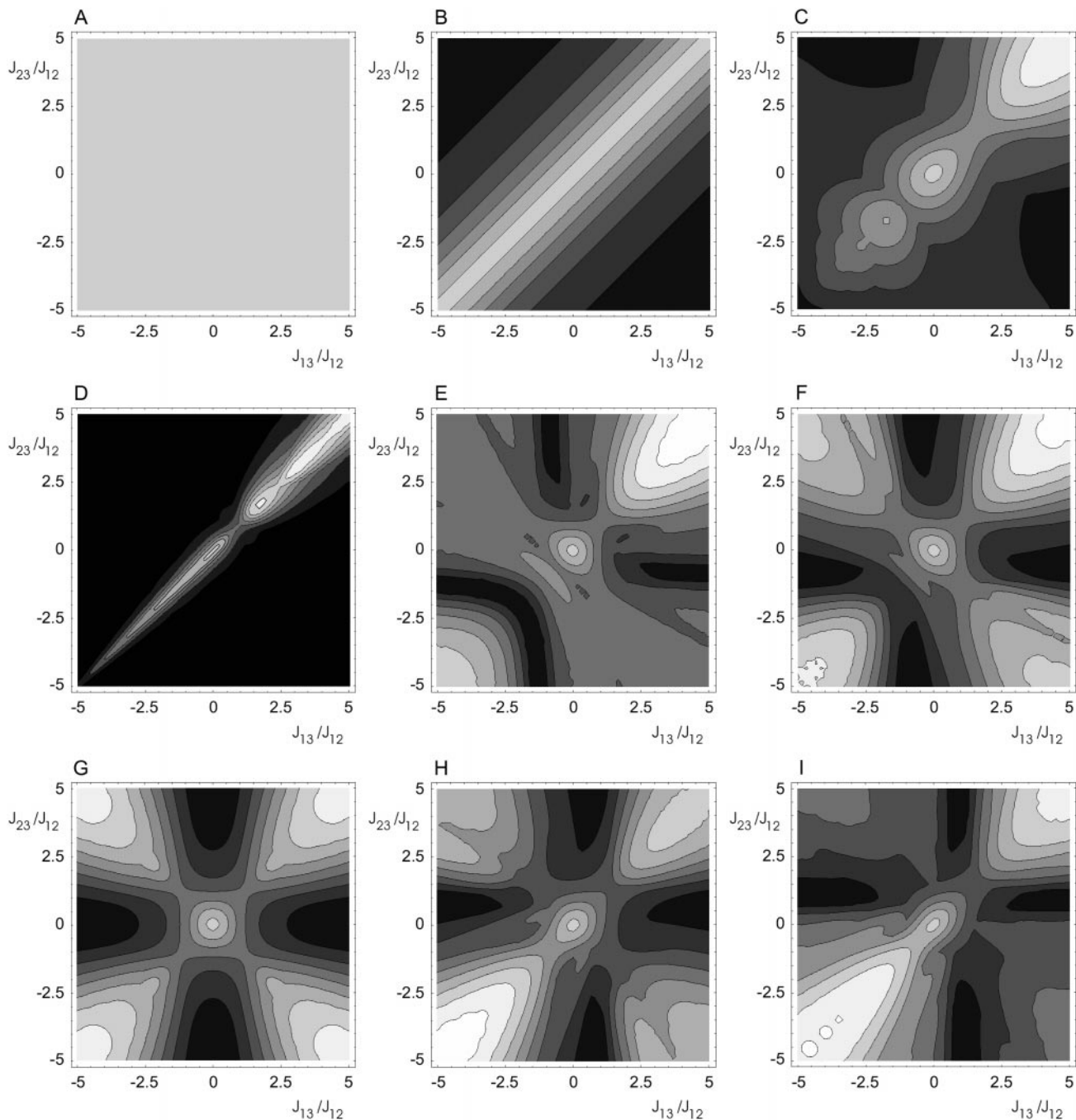


FIG. 4. Polarization transfer efficiency maps showing the quality factor $\eta_{i2}^{\hat{}}$ (Eq. [19]) as a function of the relative coupling constants J_{13}/J_{12} and J_{23}/J_{12} for a number of characteristic cases of cylindrical mixing defined by the set of planar and longitudinal scaling factors s^p and s^l (cf. Eq. [18]): (A) $s^p = \{1, 0, 0\}$, $s^l = \{1, 0, 0\}$ (corresponding to isotropic mixing for a two-spin system where $\eta_{i2} = 0.62$ [10]), (B) $s^p = \{1, 0, 0\}$, $s^l = \{1, 1, 1\}$, (C) $s^p = \{1, 0.5, 0.5\}$, $s^l = \{1, 1, 1\}$. In (D)–(R) the planar scaling factors are $s^p = \{1, 1, 1\}$ and the longitudinal scaling factors are (D) $s^l = \{5, 5, 5\}$, (E) $s^l = \{1, 1, 1\}$, (F) $s^l = \{0.5, 0.5, 0.5\}$, (G) $s^l = \{0, 0, 0\}$, (H) $s^l = \{-0.5, -0.5, -0.5\}$, (I) $s^l = \{-1, -1, -1\}$, (J) $s^l = \{-1.5, -1.5, -1.5\}$, (K) $s^l = \{-2, -2, -2\}$, (L) $s^l = \{-5, -5, -5\}$, (M) $s^l = \{1, 0, 0\}$, (N) $s^l = \{-0.5, 0, 0\}$, (O) $s^l = \{-2, 0, 0\}$, (P) $s^l = \{0, 1, 0\}$, (Q) $s^l = \{0, -0.5, 0\}$, (R) $s^l = \{0, -2, 0\}$. The contour level increment is 0.1; in black areas $0 \leq \eta_{i2}^{\hat{}} \leq 0.1$.

(effective) coupling terms exist for spin pairs 1–2 and 2–3. In practice, the maps shown in Figs. 4M–4O, 4P–4R, 5M–5O, and 5P–5R represent for example the case of heteronuclear planar mixing sequences, such as WALTZ-16 (48) or DIPSI-2 (49) applied to a spin system consisting of two homonuclear

spins with an (effective) isotropic and/or dipolar coupling tensor and one additional heteronuclear spin. For such experiments, Figs. 4M–4O and 5M–5O reflect homonuclear whereas Figs. 4P–4R and 5P–5R reflect heteronuclear transfer efficiencies.

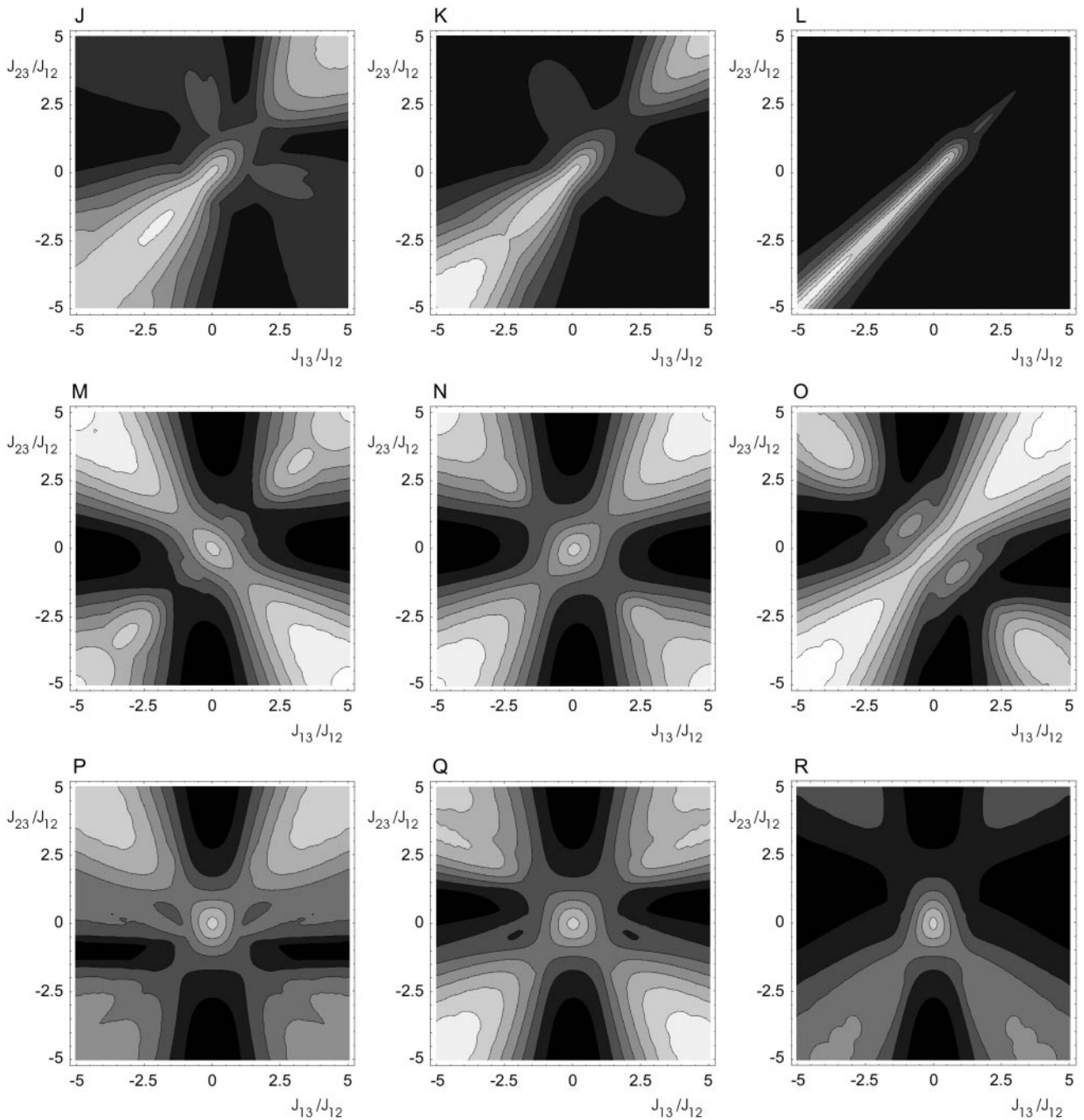


FIG. 4—Continued

CONCLUSION

For three spins 1/2, analytical polarization and coherence transfer functions were derived for general cylindrical mixing conditions, which result, e.g., from superpositions of scalar and (residual) dipolar coupling tensors. The general solutions include the special cases of dipolar, isotropic, planar, and longitudinal mixing. Whereas coherence transfer functions $T_{I_{kx} \rightarrow I_{lx}} = T_{I_{ky} \rightarrow I_{ly}}$ can also become negative (with the exception

of isotropic mixing (24, 34, 47)), only positive polarization transfer functions $T_{I_{kz} \rightarrow I_{lz}}$ were found. Based on the quality factors η_{12}^z and η_{12}^x (Eq. [19]) transfer efficiency maps were shown in Figs. 4 and 5 for special cases of interest. However, the derived analytical transfer functions also apply to the general case of Hartmann–Hahn spectroscopy of partially oriented samples, where residual dipolar coupling constants are not correlated with the size of scalar couplings and hence arbitrary ratios J_{ij}^p/J_{ij}^l are possible for each spin pair ij . In the

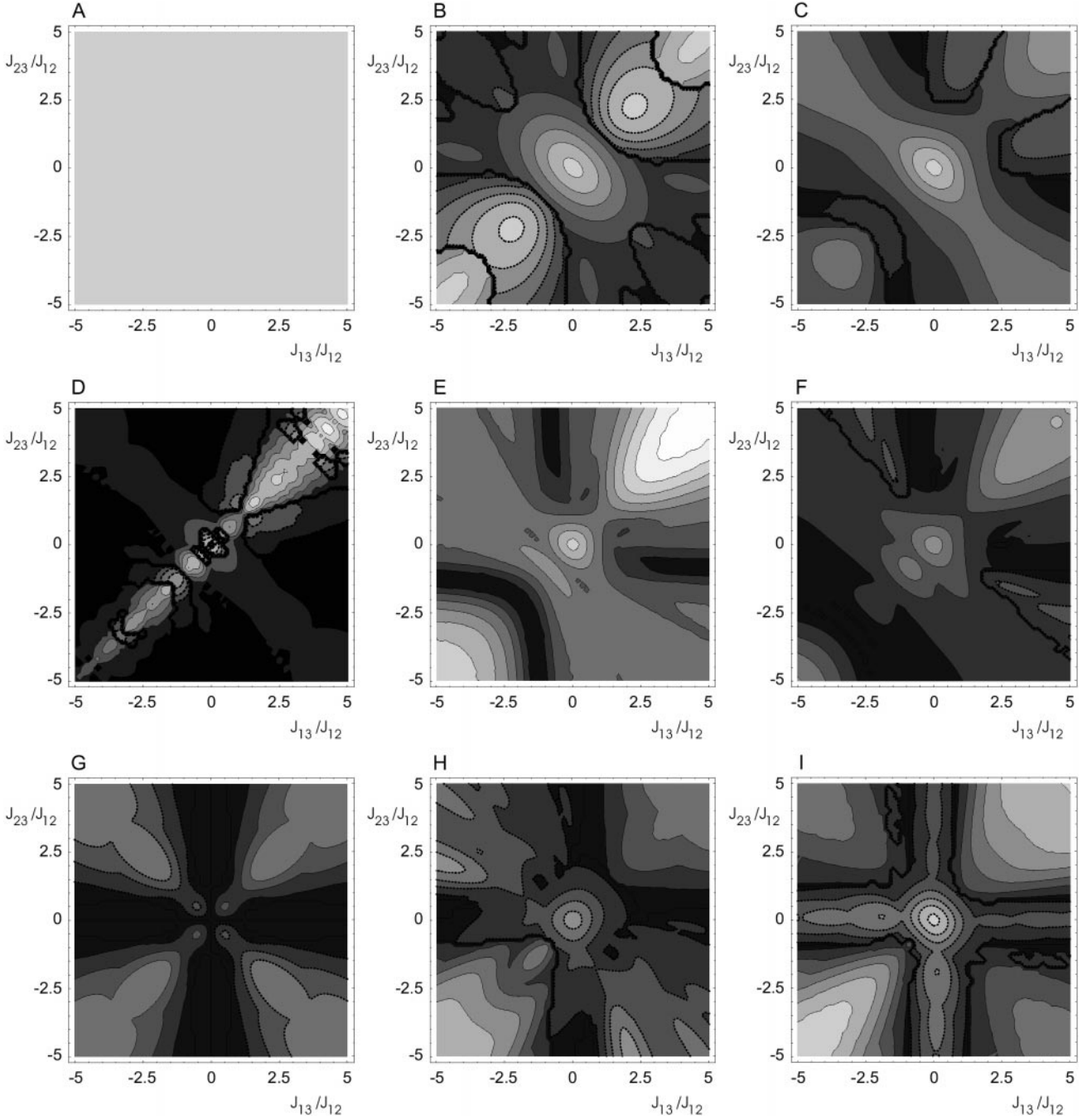


FIG. 5. Coherence transfer efficiency maps showing the quality factor $\eta_{12}^{\pm} = \eta_{12}^{\pm}$ (Eq. [19]) as a function of the relative coupling constants J_{13}/J_{12} and J_{23}/J_{12} for a number of characteristic cases of cylindrical mixing defined by the set of planar and longitudinal scaling factors \mathbf{s}^p and \mathbf{s}^l (cf. Eq. [18]): (A) $\mathbf{s}^p = \{1, 0, 0\}$, $\mathbf{s}^l = \{1, 0, 0\}$ (corresponding to isotropic mixing for a two-spin system where $\eta_{12}^{\pm} = 0.62$ [10]), (B) $\mathbf{s}^p = \{1, 0, 0\}$, $\mathbf{s}^l = \{1, 1, 1\}$, (C) $\mathbf{s}^p = \{1, 0.5, 0.5\}$, $\mathbf{s}^l = \{1, 1, 1\}$. In (D)–(R) the planar scaling factors are $\mathbf{s}^p = \{1, 1, 1\}$ and the longitudinal scaling factors are (D) $\mathbf{s}^l = \{5, 5, 5\}$, (E) $\mathbf{s}^l = \{1, 1, 1\}$, (F) $\mathbf{s}^l = \{0.5, 0.5, 0.5\}$, (G) $\mathbf{s}^l = \{0, 0, 0\}$, (H) $\mathbf{s}^l = \{-0.5, -0.5, -0.5\}$, (I) $\mathbf{s}^l = \{-1, -1, -1\}$, (J) $\mathbf{s}^l = \{-1.5, -1.5, -1.5\}$, (K) $\mathbf{s}^l = \{-2, -2, -2\}$, (L) $\mathbf{s}^l = \{-5, -5, -5\}$, (M) $\mathbf{s}^l = \{1, 0, 0\}$, (N) $\mathbf{s}^l = \{-0.5, 0, 0\}$, (O) $\mathbf{s}^l = \{-2, 0, 0\}$, (P) $\mathbf{s}^l = \{0, 1, 0\}$, (Q) $\mathbf{s}^l = \{0, -0.5, 0\}$, (R) $\mathbf{s}^l = \{0, -2, 0\}$. The contour level increment is 0.1; in black areas $|\eta_{12}^{\pm}| = |\eta_{12}^{\pm}| \leq 0.1$. Negative levels are indicated by dashed contour lines.

mixing period of homonuclear Hartmann–Hahn experiments applied to samples with residual dipolar couplings (23), WALTZ-16 (48) and DIPSI-2 (49) sequences can be used to create energy matched conditions. Similar to cw_x irradiation, these sequences create effective coupling terms that have the

form of Eq. [1] if the axis labels $\{x, y, z\}$ are replaced by $\{y, z, x\}$ and with a reduced effective dipolar coupling constant $D_{\text{eff}} = -D/2$ (50). Hence, the analytical transfer functions summarized in Tables 1, 2, and 3 are also valid for these mixing sequences if the axis labels are permuted and if in Eq.

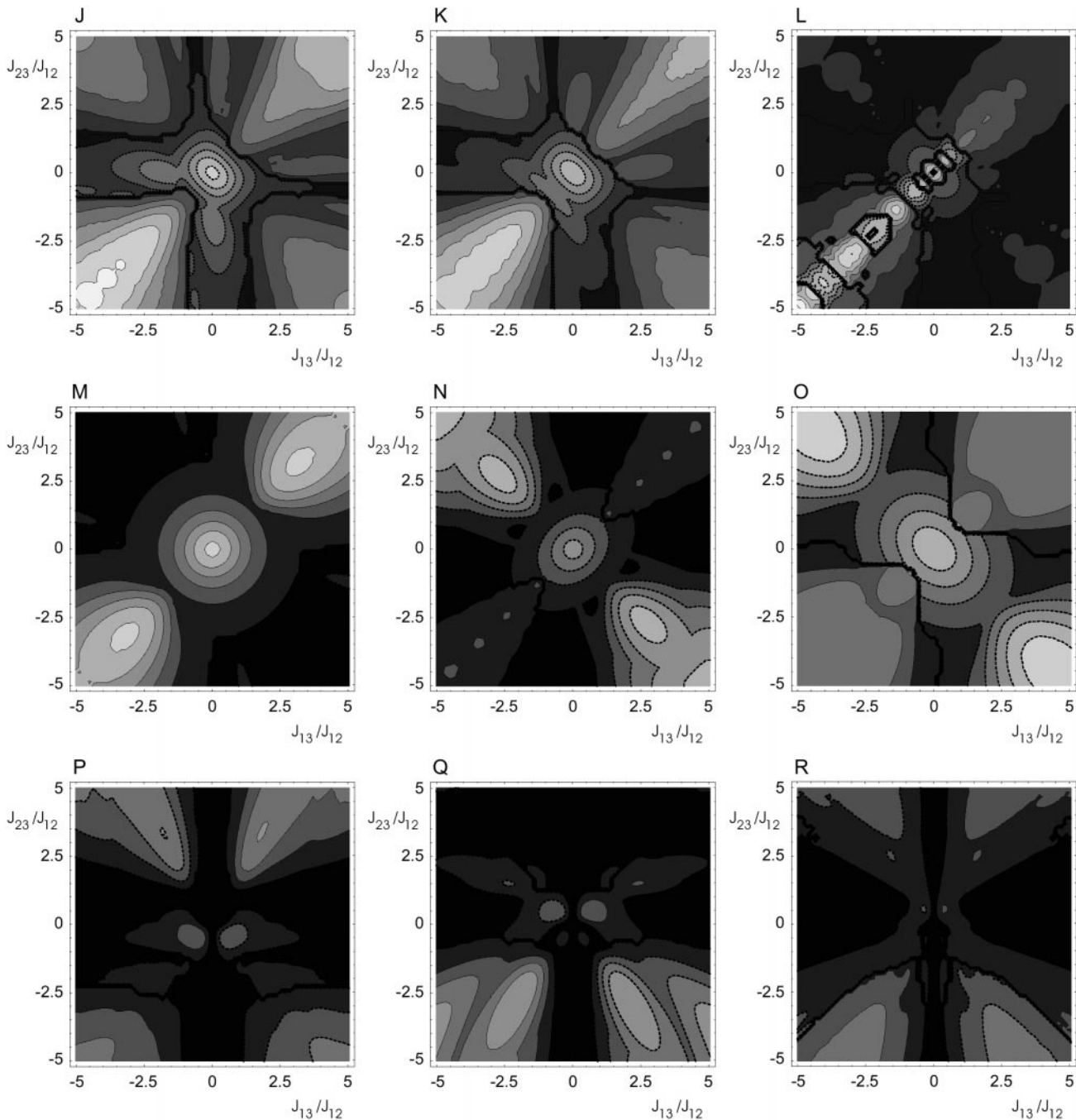


FIG. 5—Continued

[2] the dipolar coupling constants are replaced by the scaled effective dipolar coupling constants D_{eff} . It should also be kept in mind that for a given multiple-pulse sequence the form of the effective coupling tensors depends in general also on the offsets of the coupled spins (32). The derived transfer functions form a theoretical basis to understand the transfer dynamics under cylindrical mixing conditions, which are created, for example, in Hartmann–Hahn experiments in the presence of residual dipolar couplings.

ACKNOWLEDGMENTS

This work was supported by the DFG under Grant Gl 203/1-6. B.L. acknowledges a Feodor Lynen fellowship of the Alexander von Humboldt Stiftung.

REFERENCES

1. S. R. Hartmann and E. L. Hahn, Nuclear double resonance in the rotating frame, *Phys. Rev.* **128**, 2042–2053 (1962).

2. G. C. Chingas, A. N. Garroway, R. D. Bertrand, and W. B. Moniz, Zero quantum NMR in the rotating frame: J cross polarization in AX_N systems, *J. Chem. Phys.* **74**, 127–156 (1981).
3. L. Müller and R. R. Ernst, Coherence transfer in the rotating frame. Application to heteronuclear cross-correlation spectroscopy, *Mol. Phys.* **38**, 963–992 (1979).
4. A. Pines, M. G. Gibby, and J. S. Waugh, Proton-enhanced NMR of dilute spins in solids, *J. Chem. Phys.* **59**, 569–590 (1973).
5. L. Braunschweiler and R. R. Ernst, Coherence transfer by isotropic mixing: Application to proton correlation spectroscopy, *J. Magn. Reson.* **53**, 521–528 (1983).
6. A. Bax and D. G. Davis, MLEV-17-based two-dimensional homonuclear magnetization transfer spectroscopy, *J. Magn. Reson.* **65**, 355–360 (1985).
7. M. Ernst, C. Griesinger, R. R. Ernst, and W. Bermel, Optimized heteronuclear cross polarization in liquids, *Mol. Phys.* **74**, 219–252 (1991).
8. B. H. Meier, Polarization transfer and spin diffusion in solid-state NMR, in "Advances in Magnetic and Optical Resonance" (W. S. Warren, Ed.), Vol. 18, pp. 1–116, Academic Press, San Diego, 1994.
9. S. J. Glaser and J. J. Quant, Homonuclear and heteronuclear Hartmann-Hahn transfer in isotropic liquids, in "Advances in Magnetic and Optical Resonance" (W. S. Warren, Ed.), Vol. 19, pp. 59–252, Academic Press, San Diego, 1996.
10. S. J. Glaser, Coupling topology dependence of polarization-transfer efficiency in TOCSY and TACSU experiments, *J. Magn. Reson. A* **104**, 283–301 (1993).
11. D. P. Weitekamp, J. R. Garbow, and A. Pines, Determination of dipole coupling constants using heteronuclear multiple quantum NMR, *J. Chem. Phys.* **77**, 2870 (1982); Erratum, *J. Chem. Phys.* **80**, 1372 (1984).
12. P. Caravatti, L. Braunschweiler, and R. R. Ernst, Heteronuclear correlation spectroscopy in rotating solids, *Chem. Phys. Lett.* **100**, 305 (1983).
13. T. Schulte-Herbrüggen, Z. L. Mädi, O. W. Sørensen, and R. R. Ernst, Reduction of multiplet complexity in COSY-type NMR spectra. The bilinear and planar COSY experiment, *Mol. Phys.* **72**, 847–871 (1991).
14. R. Konrat, I. Burghardt, and G. Bodenhausen, Coherence transfer in nuclear magnetic resonance by selective homonuclear Hartmann-Hahn correlation spectroscopy, *J. Am. Chem. Soc.* **113**, 9135–9140 (1991).
15. Ě. Kupĉe and R. Freeman, Multiple Hartmann-Hahn coherence transfer in nuclear magnetic resonance spectroscopy, *J. Am. Chem. Soc.* **114**, 10671–10672 (1992).
16. T. Carlomagno, M. Maurer, M. Sattler, M. G. Schwendinger, S. J. Glaser, and C. Griesinger, PLUSH TACSU: Homonuclear planar TACSU with two-band selective shaped pulses applied to C^α , C' transfer and C^β , C^{aromatic} correlations, *J. Biomol. NMR* **8**, 161–170 (1996).
17. E. R. P. Zuiderweg, L. Zeng, B. Brutscher, and R. C. Morshauer, Band-selective hetero- and homonuclear cross-polarization using trains of shaped pulses, *J. Biomol. NMR* **8**, 147–160 (1996).
18. M. Shirakawa, M. Wälchli, M. Shimizu, and Y. Kyogoku, The use of heteronuclear cross-polarization for backbone assignment of ^2H -, ^{15}N - and ^{13}C -labeled proteins: A pulse scheme for triple-resonance 4D correlation of sequential amide protons and ^{15}N , *J. Biomol. NMR* **5**, 323–326 (1995).
19. O. Schedletsky, B. Luy, and S. J. Glaser, Analytical polarization and coherence transfer functions for three coupled spins 1/2 under planar mixing conditions, *J. Magn. Reson.* **130**, 27–32 (1998).
20. J. H. Prestegard, New techniques in structural NMR-anisotropic interactions, *Nature Struct. Biol.*, NMR suppl., July 1998, 517–522 (1998).
21. N. Tjandra and A. Bax, Direct measurement of distances and angles in biomolecules by NMR in a dilute liquid crystalline medium, *Science* **278**, 1111–1114 (1997).
22. M. R. Hansen, L. Mueller, and A. Pardi, Tunable alignment of macromolecules by filamentous phage yields dipolar coupling interactions, *Nat. Struct. Biol.* **5**, 1065–1074 (1998).
23. M. R. Hansen, M. Rance, and A. Pardi, Observation of long-range ^1H - ^1H distances in solution by dipolar coupling interactions, *J. Am. Chem. Soc.* **120**, 11210–11211 (1998).
24. M. Rance, Sign reversal of resonances via isotropic mixing in NMR-spectroscopy, *Chem. Phys. Lett.* **154**, 242–247 (1989).
25. M. L. Remerowski, S. J. Glaser, and G. P. Drobny, A theoretical study of coherence transfer by isotropic mixing: Calculation of pulse sequence performance for systems of biological interest, *Mol. Phys.* **68**, 1191–1218 (1989).
26. J. Cavanagh, W. J. Chazin, and M. Rance, The time dependence of coherence transfer in homonuclear isotropic mixing experiments, *J. Magn. Reson.* **87**, 110–131 (1990).
27. A. Bax, G. M. Clore, and A. M. Gronenborn, ^1H - ^1H correlation via isotropic mixing of ^{13}C magnetization, a new three-dimensional approach for assigning ^1H and ^{13}C spectra of ^{13}C -enriched proteins, *J. Magn. Reson.* **88**, 425–431 (1990).
28. H. L. Eaton, S. W. Fesik, S. J. Glaser, and G. P. Drobny, Time dependence of ^{13}C - ^{13}C magnetization transfer in isotropic mixing experiments involving amino acid spin systems, *J. Magn. Reson.* **90**, 452–463 (1990).
29. S. J. Glaser and G. P. Drobny, Assessment and optimization of pulse sequences for homonuclear isotropic mixing, in "Advances in Magnetic Resonance" (W. S. Warren, Ed.), Vol. 14, pp. 35–58, Academic Press, New York, 1990.
30. S. S. Wijmenga, H. A. Heus, B. Werten, G. A. van der Marel, J. H. van Boom, and C. W. Hilbers, Assignment strategies and analysis of cross-peak pattern and intensities in the three-dimensional homonuclear TOCSY-NOESY of RNA, *J. Magn. Reson. B* **103**, 134–141 (1994).
31. R. Brüschweiler and R. R. Ernst, A cog-wheel model for nuclear-spin propagation in solids, *J. Magn. Reson.* **124**, 122–126 (1997).
32. F. Kramer, B. Luy, S. J. Glaser, Offset dependence of homonuclear Hartmann-Hahn transfer based on residual dipolar couplings in solution state NMR, *Appl. Magn. Reson.* **17**, 173–187 (1999).
33. D. M. Taylor and A. Ramamoorthy, Analysis of dipolar-coupling-mediated coherence transfer in a homonuclear two spin-1/2 solid-state system, *J. Magn. Reson.* **141**, 18–28 (1999).
34. O. Schedletsky and S. J. Glaser, Analytical coherence-transfer functions for the general AMX spin system under isotropic mixing, *J. Magn. Reson. A* **123**, 174–180 (1996); Erratum, *J. Magn. Reson.* **136**, 134 (1999).
35. B. Luy and S. J. Glaser, Analytical polarization and coherence transfer functions for three dipolar coupled spins 1/2, *J. Magn. Reson.* **142**, 280–287 (2000).
36. B. Luy, O. Schedletsky, and S. J. Glaser, Analytical polarization transfer functions for four coupled spins 1/2 under isotropic mixing conditions, *J. Magn. Reson.* **138**, 19–27 (1999).
37. A. Majumdar, Analytical expressions for isotropic mixing in three- and four-spin topologies in ^{13}C systems, *J. Magn. Reson. A* **121**, 121–126 (1996).
38. J. C. Bonner and M. E. Fisher, Linear magnetic chains with anisotropic coupling, *Phys. Rev.* **135**, A640–A658 (1964).
39. E. Ising, Beitrag zur Theorie des Ferromagnetismus, *Z. Physik* **31**, 253–258 (1925).

40. W. J. Caspers, "Spin Systems," World Scientific, London, 1989.
41. O. Kahn, "Molecular Magnetism," VCH Publishers, New York, 1993.
42. E. H. Lieb, T. Schultz, and D. C. Mattis, Two soluble models of an antiferromagnetic chain, *Ann. Phys. (Paris)* **16**, 407–466 (1961).
43. F. Bloch, Zur Theorie des Ferromagnetismus, *Z. Physik* **61**, 206 (1930).
44. R. R. Ernst, G. Bodenhausen, and A. Wokaun, "Principles of Nuclear Magnetic Resonance in One and Two Dimensions," Oxford Univ. Press, Oxford, 1987.
45. I. N. Bronshtein, K. A. Semendyayew, "Handbook of Mathematics," Verlag Harri Deutsch, Frankfurt, 1985.
46. A. Wolfram, Mathematica. "A System for Doing Mathematics by Computer," Addison-Wesley, Redwood City, CA, 1988.
47. B. Luy and S. J. Glaser, Negative polarization transfer between a spin 1/2 and a spin 1, *Chem. Phys. Lett.* **323**, 377–381 (2000).
48. A. J. Shaka, J. Keeler, T. Frenkiel, and R. Freeman, An improved sequence for broadband decoupling: WALTZ-16, *J. Magn. Reson.* **52**, 335–338 (1983).
49. A. J. Shaka, C. J. Lee, and A. Pines, Iterative schemes for bilinear operators; application to spin decoupling, *J. Magn. Reson.* **77**, 274–293 (1988).
50. P. Robyr, B. H. Meier, and R. R. Ernst, Radio-frequency-driven nuclear spin diffusion in solids, *Chem. Phys. Lett.* **162**, 417–423 (1989).